CHEMPHYSCHEM

DOI: 10.1002/cphc.201000531

Electroluminescence from Individual Pentacene Nanocrystals

Alexander Kabakchiev,*[a] Klaus Kuhnke,[a] Theresa Lutz,[a] and Klaus Kern[a, b]

Pentacene is a promising candidate for use in organic and optoelectronic devices. The electronic properties and structures of the organic semiconductor have been extensively studied for thin films and macroscopic crystals. Herein, we report the first electroluminescence measurements from single pentacene nanocrystals using the tip of a scanning tunneling microscope (STM) as a local electrode. For localized charge injection by the STM tip, strongly red-shifted luminescence at the bulk exciton energies is observed. The emission from delocalized excitations and missing features from individual molecules reflects significant intermolecular coupling. Excitation and emission mechanism are discussed based on the observed dependence on electrical and structural parameters.

Organic semiconductors have made a strong entrance in nanoscale electronics and optoelectronics during the last decade. Pentacene has become the prime model system to explore the physical principles and the technological challenges associated with organic devices.[1] The extended conjugation and a favorable crystal structure are responsible for its success as organic semiconductor. On the single-molecule level pentacene has also become the gold standard of local scanning probe imaging and spectroscopy. Impressive results through the use of STM[2,3] and atomic force microscopy (AFM)[4] demonstrate submolecular imaging capabilities and realize experimental conditions in which the single organic molecule preserves its structural and electronic features. Gas-phase-like electronic orbitals can, for example, be observed on a molecule adsorbed on an insulator. On the other hand, these studies show that the position and width of electronic levels are determined by their environment. Making the step from the isolated molecule to a small isolated molecular solid opens up a way to address interactions between identical molecules. Molecular crystals are bound together by weak van der Waals forces and can also preserve properties of their molecular building blocks to a large extent. They can be described in a first approximation by an "oriented gas" model.[5] Essential for this study, however, is the fact that crystalline pentacene exhibits an intermolecular coupling which is comparatively strong for this class of materials. The resulting electronic dispersion becomes largest along the direction of overlap between π orbitals of neighboring molecules.[6–9] Pentacene is thus a material well-suited to explore consequences of intermolecular coupling on the optical emission from the low energy electronic excitations.

Herein we employ scanning tunneling microscopy and spectroscopy at 4.2 K to study charge carrier excitation and electroluminescence of individual pentacene molecules and nanocrystals with submolecular resolution. STM-induced luminescence has proven its ability to obtain optical spectra from isolated molecules[10,11] and from thin molecular films.[12–17] We report on the first STM-induced luminescence from an acene. The method allows the local characterization of molecular structure, orientation, and the identification of the excited species according to their optical spectra. In combination with electronic spectroscopy and measurements of the electrical parameters for luminescence it can provide a detailed scheme of excitation and emission processes.[18] The STM tip injects charges locally into the molecular top layer. This suggests that luminescence may predominantly be emitted by a single molecule situated below the tip. This has, in fact, been confirmed in earlier studies of STM-induced luminescence on organic solids.[13,14,17,19] In contrast, herein the emission line is strongly red-shifted with respect to the emission of matrix-embedded single pentacene molecules. This indicates strong intermolecular coupling and emission from a delocalized excitation. As a result, the observed luminescence spectrum is very robust and becomes independent of the point of charge injection. The pentacene nanocrystal acts already as a molecular crystal, coupled to its top and bottom electrodes through tunnel junctions instead of Schottky contacts. It represents a bulk-like light source at the limit of small dimensions.

Samples were prepared and studied in ultrahigh vacuum (UHV). As substrates we used noble metal single crystals. The crystal surfaces of Au(111), Ag(111) and Cu(111) were cleaned in situ by Ar^+ sputtering and annealing. Subsequently, 1–2 ML (monolayer) of KCl were deposited by thermal evaporation. Pentacene nanocrystals were grown on top of these substrates in a two-step process. First, highly purified pentacene was thermally evaporated on the sample held at a low temperature ($T < 90$ K). The evaporation rate was low to yield a coverage of about 1 ML during 5 min evaporation time. The result is a dispersed arrangement of pentacene molecules adsorbed flat on the KCl layer. Subsequently, the substrate was annealed to 220 K for 1 min and transferred into the STM operated at 4.2 K. The annealing step leads to pentacene dewetting on the KCl layer and to the formation of molecularly ordered three-dimensional pentacene crystallites a few nanometers high with lateral dimensions of a few tens of nanometers. No pentacene remains in between the nanocrystals. We find that the molecular nanocrystals nucleate at step edges, which are either due to a step in the KCl layer or a step of the metal substrate covered in a carpet-like fashion by the KCl layer. As STM tips we em-

[a] A. Kabakchiev, Dr. K. Kuhnke, T. Lutz, Prof. Dr. K. Kern
Max-Planck Institut für Festkörperforschung
Heisenbergstr. 1, 70569 Stuttgart, (Germany)
Fax: (+49) 711-689-1662
E-mail: a.kabakchiev@fkf.mpg.de

[b] Prof. Dr. K. Kern
Institut de Physique de la Matière Condensée
Ecole Polytechnique Fédérale de Lausanne (EPFL)
1015 Lausanne (Switzerland)

ployed electrochemically etched gold[20] and tungsten tips. Ag tips were prepared inside the UHV chamber by coating of etched tungsten tips with a thin Ag layer. Prior to the measurements on pentacene the tips were conditioned on a clean metal substrate and checked for their spectroscopic and imaging performance. Luminescence from the tunnel junction is collected by a N.A. = 0.41 aspheric lens placed a few millimeters away from the STM tip. The light propagates as a free collimated beam inside the vacuum and exits the UHV chamber through a glass window. The setup avoids any significant heat input in the opposite direction from the room-temperature environment. Spectra were recorded by an Acton Research Spectra Pro 300i Spectrograph using a 150 lines inch^{-1} blazed grating and a Peltier-cooled CCD camera behind a light intensifier.

Individual pentacene nanocrystals 3–15 layers thick with lateral dimensions of a few tens of namometres were grown on top of an ultra-thin KCl layer on a metal substrate. When not stated otherwise herein, the substrate is a single-crystal Au(111) surface. The KCl layer acts as a tunnel barrier because its large bulk band gap is higher than 7 eV[21] and its high dielectric constant provides only a small voltage drop in the external electric field of the tunnel junction. The vacuum gap between STM tip and crystal surface defines a second (tunable) tunnel barrier. In this geometry (Figure 1 a) we obtained submolecular resolution of pentacene molecules on top of the crystal and in some cases also at the steep sides of the crystals. The nanocrystals exhibit a high molecular order with translational symmetry in which structural defects are sometimes found. The topography at the nanocrystal surface and the measured crystal heights allow us to determine the nanocrystal structure (Figures 1 c,d). The lattice parameters with respect to the surface are listed in Table 1. At negative bias voltage the surface molecules are imaged through their highest occupied molecular orbital (HOMO), identified by its five nodes of the electronic wave function parallel to the intermediate molecular axis (Figure 1 d). For comparison we show the STM topograph of the HOMO orbital of an isolated pentacene molecule adsorbed flat on the KCl layer (Figure 1 b). The pentacene molecules in the nanocrystal layers are orientated with their long axis parallel to the surface and the molecular plane rotated by

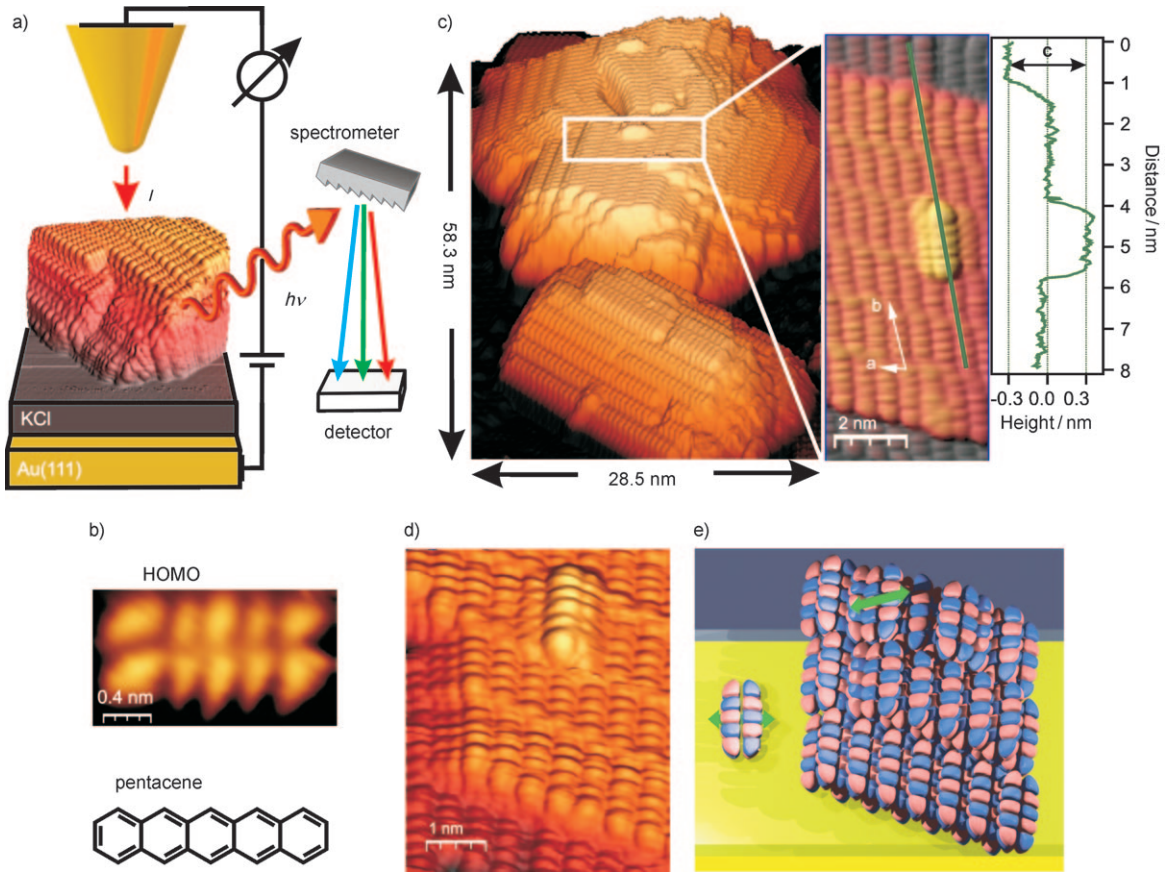

Figure 1. Experiment and pentacene nanocrystal structure. a) Principle of the experiment: The tip of an STM is positioned above a pentacene nanocrystal (colored black–yellow) for imaging and tunneling spectroscopy. A tunnel current is injected into the nanocrystal decoupled from the Au(111) substrate by an ultrathin KCl layer. The emitted luminescence light is detected by an optical spectrometer. b) Chemical structure (bottom) of pentacene and its HOMO orbital (top) imaged by STM for a molecule adsorbed on the KCl layer on Au(111) (U = −2.4 V, I = 10 pA). c) STM topographic image in 3D presentation of a pentacene nanocrystal on KCl/Cu(111) and detail (right) in top view. The in-plane lattice vectors **a** and **b** are drawn in the topograph. The layer height is indicated in the height profile (green line). d) Detail of the nanocrystal with two visible layers and an admolecule. e) Model of a structure similar to (d) using a cartoon-like presentation of the HOMO orbitals with different signs of the electronic wavefunction indicated in blue and red. Left: Top view of a flat-lying single molecule. The green arrows indicate the orientation of the transition-dipole vector for an excitation derived from transitions between LUMO and HOMO orbital. The measurements are presented using the WSxM software.[36]

Table 1. Structure parameters of the pentacene nanocrystal. Note that the value c corresponds to twice the measured layer height as successive layers have different molecular orientations.

Lattice Vector lengths	**a** =	0.63 ± 0.03 nm
	b =	1.58 ± 0.04 nm
	c =	0.62 ± 0.1 nm
Angles	angle (**a**,**b**) =	69 ± 3°
	angle (long mol.axis,**b**) =	4 ± 2°

approximately 26° with respect to the surface plane. This rotation is evidenced by the fact that the node of the HOMO orbital along the long axis of the molecule is not seen on the closed layer, but only for admolecules and step edges (Figures 1 c,d). The cartoon in Figure 1 e, which models a structure similar to that shown in Figure 1 d, illustrates that the rotation leads to a short **a** vector between neighboring molecules and hides the longitudinal node of the orbital from observation by the STM tip. We remark that the imaging STM tip is separated from the molecular top layer through a vacuum tunnel gap of the order of 0.5–1.0 nm and thus only the lobes of the electronic wave function extending into the vacuum become observable. Within experimental accuracy (Figure 1 e) the nanocrystals realize the pentacene bulk lattice structure.[22] The strong local variations do, however, not allow one to distinguish between two distinct lattices obtained by growth from solution or growth by vapor deposition.[23] The nanocrystal is markedly different from known structures of thin films on insulators on which layers are formed by molecules standing upright.[6,24]

STM-induced luminescence spectra are plotted in Figure 2. The upper row presents luminescence spectra recorded with the STM tip positioned on a pentacene nanocrystal for different tip materials and close-packed single-crystal surfaces of different metals. The dominating peak in these spectra is situated at 1.6 eV. Spectra recorded next to these nanocrystals with the STM tip positioned above the ultrathin KCl insulator layer are shown for comparison in the lower row. The features in these spectra are due to tip-induced plasmons localized between metallic tip and metallic substrate and depend on tip shape and tip and substrate material.[25] We emphasize that the two corresponding spectra in each column exhibit no similar features. Moreover, we find that the nanocrystal spectra in the upper row are well reproduced and the peak positions do not depend on the underlying plasmonic spectrum. We conclude that STM-induced luminescence allows to access optical spectra originating from the pentacene nanocrystals. Comparing the three typical spectra in the upper row of Figure 2 to pentacene luminescence spectra in the literature, we find agreement only with photoluminescence spectra from macroscopic single crystals measured at 8 K.[26] There is no match with the lowest singlet transition of individual pentacene molecules, which is situated at 2.30 eV for the isolated molecule,[27,28] red-shifted by dielectric screening to 2.03 eV when embedded in *p*-terphenyl[29] and to 1.98 eV for embedding in tetracene.[30] Pentacene electroluminescence spectra recorded from organic field-effect transistor devices exhibit typically broad spectral features extending to energies above 2 eV.[31] The low temperature in our study provides sharp features, and the geometry of charge transport along the shortest crystal dimension suppresses the influence of domain boundaries with respect to thin-film geometries. Optically induced luminescence from organic crystals probes bulk properties with surface contributions being negligible. In contrast, nanocrystals provide a high surface-to-volume ratio. The agreement of our data with single-crystal photoluminescence is thus surprisingly good. It concerns peak energy, peak width, peak asymmetries and the relative peak heights. Apart from the strong peak at 1.59 eV, a shoulder around 1.45 eV is found. In addition, a small peak at 1.76 eV can be identified which only sometimes exceeds the noise level in our spectra. Following the discussions in refs. [26,32] we can assign the observed features to the free singlet exciton (1.78 eV), the self-trapped exciton (1.64 eV), and an impurity related line (ca. 1.4–1.5 eV). The dominance of the

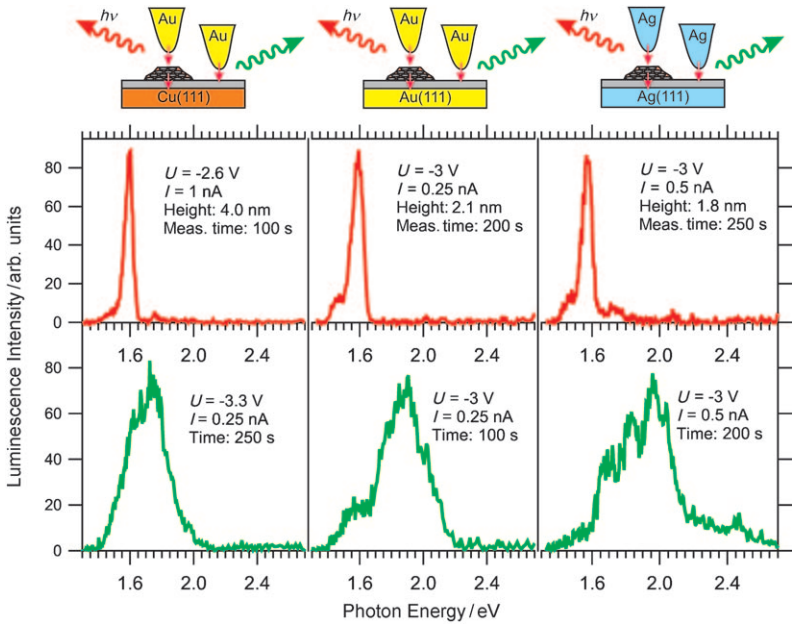

Figure 2. STM-induced electroluminescence. Top: Drawing of the experiments shown in the color-coded spectra below. Upper row of spectra: STM-induced luminescence recorded for the STM tip positioned on the pentacene nanocrystals with the listed crystal height, spectral measuring time and tunneling parameters: bias voltage (*U*) and current (*I*). Lower row of spectra: STM-induced luminescence due to tip-induced plasmons recorded with the STM tip positioned on the KCl-covered single-crystal surface.

1.6 eV peak can be regarded as characteristic for crystals in contrast to the 1.8 eV peak dominating for pentacene clusters and thin films.[33] Pentacene-related luminescence could only be observed at negative bias voltage and for crystallites of a minimum thickness of 1.5 nm. As the reduced dimension of the crystallites suggest a spatial exciton confinement we analyzed the peak position of the 1.6 eV line with respect to crystal width and height. A shift of peak energy could, however, not be identified within experimental accuracy and is estimated to be smaller than ca. 10 meV over the range of 1.5–4.0 nm crystal thickness. While a theoretical estimate on the confinement is not available, the assignment to a self-trapped Frenkel exciton may rationalize the small effect.

A closer inspection of the features in the STM-induced luminescence spectra finds consistent red-shifts of approximately 40 meV with respect to a 8 K photoluminescence spectrum.[26] We find that a significant part of the shift is related to the electric field between tip and sample which is of the order 1 V nm^{-1}. The shift of the peak energy of the strongest spectral feature between −3 V and −2 V bias voltage reaches almost 10 meV. This shift is remarkable and challenges the assignment of the feature to a pure Frenkel-type exciton. A detailed discussion of the Stark shift is, however, beyond the scope of this paper and will be presented in detail in a forthcoming publication.

The dependence of luminescence intensity of the 1.6 eV peak on the electric parameters is plotted in Figures 3 b,c. The emission is linear in tunnel current and shows an onset near 1.8 V bias voltage. The small energetic difference between onset and main emission line indicates only small losses before exciton formation. An onset even below the bulk transport threshold of pentacene (2.2 eV[34]) suggests the creation of excitons close to the position of charge injection. Electron tunneling spectra measured on single pentacene molecules on the KCl layer (Figure 3 a) yield charge injection potentials of −2.4 eV for the HOMO and +2.0 eV for the LUMO. The current between the HOMO and LUMO onsets vanishes already for pentacene in the first layer on the KCl buffer. This demonstrates the decoupling of the electronic states of metal and molecule. Independent of this decoupling the HOMO and LUMO levels shift only weakly with bias voltage and changing tip–molecule separation[2] as the KCL layer is thin and exhibits a high dielectric constant. The nanocrystal tunneling spectra (Figure 3 a) are offset with respect to single molecule spectra by about 1 eV to more positive voltage. This shift cannot be due to the STM-related electric field inside the pentacene because the shift is towards higher energies also at negative bias. We attribute the offset to band formation in the crystal and a reduction of work function.

Based on the results presented, we propose a scenario leading from charge injection to luminescence in the pentacene nanocrystals: The observed onset bias of luminescence at −1.8 eV (Figure 3 c) suggests that after extraction of an electron by the tip, an exciton (1.78 eV) is formed. A weak signature of its decay is observed in the luminescence. At higher bias voltage additional channels may open up. Following the assignment of transitions in the literature[26] the 1.78 eV exciton is mobile within the crystal. By self-trapping the exciton becomes immobilized, losing about 0.2 eV. This exciton provides the dominant signal. Figure 3 d sketches an energy diagram of the electronic levels involved in the electroluminescence near its onset. The Au electrodes inject charge carriers through their respective tunnel junctions. The electrical conductance required by STM operation is provided by the valence band. A bulk-like conduction band cannot line up with the substrate Fermi energy. Due to the low temperature in the experiment, the electrons are injected through an extended tunnel barrier which may favor a direct exciton formation from the continuous current of holes in the valence band. The substrate Fermi energy is closer to the conduction band edge than to the va-

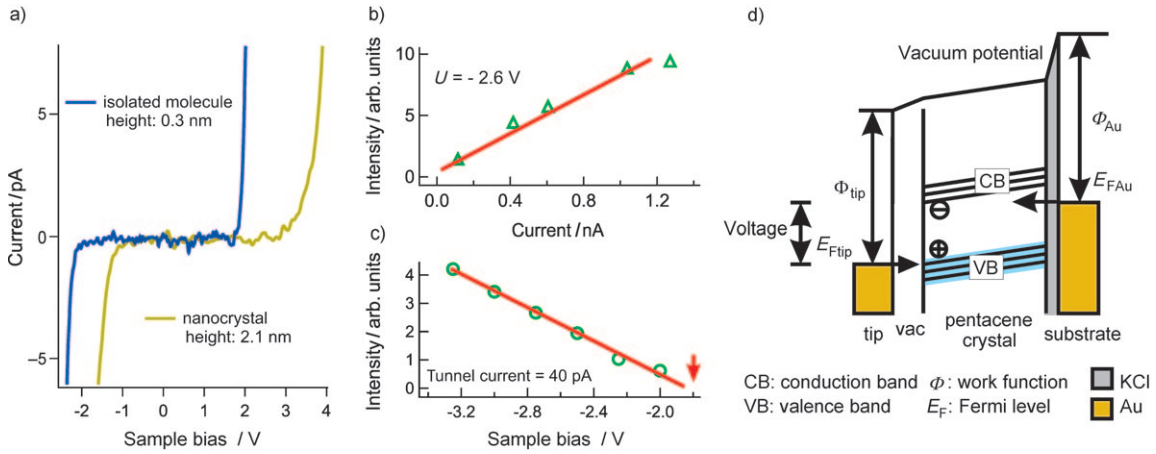

Figure 3. Electronic properties. a) Tunnel current as a function of bias voltage [Au(111) substrate with respect to STM Au tip] measured on an isolated molecule (blue) and on a nanocrystal (yellow). b) Integrated STM luminescence intensity from a nanocrystal as a function of tunnel current for constant bias voltage. c) Integrated-STM-induced luminescence as a function of bias voltage for constant tunnel current, luminescence collection time per point: 250 s. d) Electronic level diagram for the charge-injection geometry employed for the measurements with the bias voltage near the luminescence onset: Vacuum potential (top line), electronic levels of the metals and pentacene band structure. The two tunnel barriers are symbolized by the gray (KCl layer) and the white (vacuum) gap.

lence band edge (Figure 3d). This and the differences of electron and hole mobilities can account for the fact that light emission is observed only at negative bias.

An important aspect for the understanding of the luminescence mechanism is the absence of observable molecular luminescence from isolated pentacene molecules on the insulating layer. Only for nanocrystals reaching a thickness of 1.5 nm STM-induced intrinsic luminescence from pentacene was strong enough to become detectable. From the position of electronic states of the isolated molecule (Figure 3a) the creation of electron–hole pairs should also be possible for hole injection into the isolated molecule if we assume its HOMO–LUMO transition at or below 2.1 eV. Two mechanisms may be responsible for the different behavior of crystal and single molecule: First, the generation of luminescence inside the nanocrystal can provide a relatively large spatial separation of the decaying exciton from the adjacent metal electrodes. Emission close to metal surfaces is known to lead to efficient nonradiative quenching for example, due to electron–hole pair generation in the metal (ref. [35] and references therein). Second, single molecules adsorb flat on the surface while pentacene molecules in the crystal are rotated around their long axis. The transition dipole of HOMO–LUMO-derived transitions is oriented along the intermediate molecular principal axis as indicated by the double-headed green arrows in Figure 1e for pentacene on the substrate and in the crystal. The radiation from a flat-lying molecule is efficiently screened by the metal substrate and can in addition not couple well to tip-induced plasmonic modes. The efficiency of radiation into the detected far field becomes significantly increased through tip enhancement.[17,19] As the second mechanism, however, would not apply for the suppression of luminescence for very thin crystals the first mechanism appears to be decisive herein.

In conclusion, our experiments demonstrate STM-induced luminescence from an acene. Luminescence from delocalized excitons can be obtained even for highly localized injection of charge carriers from an STM tip. The interaction between neighboring molecules provides a sufficient delocalization of the excitation to yield bulk-like emission spectra. The suppression of luminescence for ultrathin crystals suggests emission from the nanocrystal at sufficiently large distance (>1 nm) from the metallic electrodes. The crystal structure can affect the emission conditions through the orientation of the emitting transition dipole. The experimental setup employed herein realizes an organic light source made of a homogeneous material with bulk properties near its lower size limit. The results can provide a basis for studies to explore new functionalities by employing layered organic structures or single molecules embedded in host nanocrystals.

Acknowledgements

We thank Prof. J. Wrachtrup and Prof. J. Pflaum for valuable discussions and the supply with purified pentacene powder.

Keywords: exciton · luminescence · nanostructures · pentacene · scanning probe microscopy

[1] M. Kitamura, Y. Arakawa, *J. Phys. Condens. Matter* **2008**, *20*, 184011.
[2] J. Repp, G. Meyer, S. M. Stojkovic, A. Gourdon, C. Joachim, *Phys. Rev. Lett.* **2005**, *94*, 026803.
[3] W.-H. Soe, C. Manzano, A. DeSarkar, N. Chandrasekhar, C. Joachim, *Phys. Rev. Lett.* **2009**, *102*, 176102.
[4] L. Gross, F. Mohn, N. Moll, P. Liljeroth, G. Meyer, *Science* **2009**, *325*, 1110.
[5] M. Schwoerer, H. C. Wolf, *Organic Molecular Solids*, Wiley-VCH, **2007**.
[6] C. D. Dimitrakopoulos, A. R. Brown, A. Pomp, *J. Appl. Phys.* **1996**, *80*, 2501.
[7] H. Klauk, M. Halik, U. Zschieschang, G. Schmid, W. Radlik, W. Weber, *J Appl. Phys.* **2002**, *92*, 5259.
[8] H. Kakuta, T. Hirahara, I. Matsuda, T. Nagao, S. Hasegawa, N. Ueno, K. Sakamoto, *Phys. Rev. Lett.* **2007**, *98*, 247601.
[9] S. Berkebile, P. Puschnig, G. Koller, M. Oehzelt, F. P. Netzer, C. Ambrosch-Draxl, M. G. Ramsey, *Phys. Rev. B* **2008**, *77*, 115312.
[10] W. Deng, D. Fujita, T. Ohgi, *J. Chem. Phys.* **2002**, *117*, 4995.
[11] X. H. Qiu, G. V. Nazin, W. Ho, *Science* **2003**, *299*, 542.
[12] R. Berndt, R. Gaisch, W. D. Schneider, J. K. Gimzewski, B. Reihl, R. R. Schlittler, M. Tschudy, *Appl. Phys. A* **1993**, *57*, 513.
[13] Z. C. Dong, X. L. Guo, A. S. Trifonov, P. S. Dorozhkin, K. Miki, K. Kimura, S. Yokoyama, S. Mashiko, *Phys. Rev. Lett.* **2004**, *92*, 086801.
[14] E. Ćavar, M.-C. Blüm, M. Pivetta, F. Patthey, M. Chergui, W.-D. Schneider, *Phys. Rev. Lett.* **2005**, *95*, 196102.
[15] H. W. Liu, Y. Ie, R. Nishitani, Y. Aso, H. Iwasaki, *Phys. Rev. B* **2007**, *75*, 115429.
[16] D. Ino, T. Yamada, M. Kawai, *J. Chem. Phys.* **2008**, *129*, 014701.
[17] Z. C. Dong, X. L. Zhang, H. Y. Gao, Y. Luo, C. Zhang, L. G. Chen, R. Zhang, X. Tao, Y. Zhang, J. L. Yang, J. G. Hou, *Nat. Photonics* **2010**, *4*, 50.
[18] S. W. Wu, G. V. Nazin, W. Ho, *Phys. Rev. B* **2008**, *77*, 205430.
[19] F. Rossel, M. Pivetta, F. Patthey, W.-D. Schneider, *Optics Express* **2009**, *17*, 2714.
[20] B. Ren, G. Picardi, B. Pettinger, *Rev. Sci. Instrum.* **2004**, *75*, 837.
[21] T. Tomiki, *J. Phys. Soc. Jpn* **1967**, *22*, 463.
[22] C. C. Mattheus, A. B. Dros, J. Baas, A. Meetsma, J. L. de Boer, T. T. M. Palstra, *Acta Crystallogr. C* **2001**, *57*, 939.
[23] M. L. Tiago, J. E. Northrup, S. G. Louie, *Phys. Rev. B* **2003**, *67*, 115212.
[24] L. Ruppel, A. Birkner, G. Witte, C. Busse, T. Lindner, G. Paasch, C. Woll, *J. Appl. Phys.* **2007**, *102*, 033708.
[25] R. Berndt, J. K. Gimzewski, P. Johansson, *Phys. Rev. Lett.* **1991**, *67*, 3796.
[26] R. He, X. Chi, A. Pinczuk, D. V. Lang, A. P. Ramirez, *Appl. Phys. Lett.* **2005**, *87*, 211117.
[27] E. Heinecke, D. Hartmann, A. Hese, *J. Chem. Phys.* **2003**, *118*, 113.
[28] R. Lehnig, A. Slenczka, *J. Chem. Phys.* **2005**, *122*, 244317.
[29] U. P. Wild, F. Guttler, M. Pirotta, A. Renn, *Chem. Phys. Lett.* **1992**, *193*, 451.
[30] W. E. Geacintov, J. Burgos, I. M. Pope, C. Strom, *Chem. Phys. Lett.* **1971**, *11*, 504.
[31] M. Schidleja, C. Melzer, H. von Seggern, *Appl. Phys. Lett.* **2009**, *94*, 123307.
[32] T. Aoki-Matsumoto, K. Furuta, T. Yamada, H. Moriya, K. Mizuno, *Int. J. Mod. Phys. B* **2001**, *15*, 3753.
[33] R. He, N. G. Tassi, G. B. Blanchet, A. Pinczuk, *Appl. Phys. Lett.* **2005**, *87*, 103107.
[34] D. V. Lang, X. Chi, T. Siegrist, A. M. Sergent, A. P. Ramirez, *Phys. Rev. Lett.* **2004**, *93*, 086802.
[35] K. Kuhnke, R. Becker, M. Epple, K. Kern, *Phys. Rev. Lett.* **1997**, *79*, 3246.
[36] I. Horcas, R. Fernandez, J. M. Gomez-Rodriguez, J. Colchero, J. Gomez-Herrero, A. M. Baro, *Rev. Sci. Instrum.* **2007**, *78*, 013705.

Received: July 1, 2010
Published online on October 28, 2010

